

Influence of Contact Friction on Force-Deflection of Orthodontic NiTi Archwire: A Computational Study

M. F. Razali and A. S. Mahmud

Abstract

The force response of NiTi archwire with respect to tooth movement in orthodontic leveling treatment depends largely on the sliding resistance of a bracket system. This study investigated the influence of contact friction between the wire and the bracket towards the force-deflection behavior of superelastic NiTi wire. A finite-element model of a three-bracket bending configuration was developed, and a user material subroutine was employed to predict the force response. The archwire was bent to a certain displacement representing the curvature of the wire when installed in a patient, and the coefficient of contact friction with the brackets was defined at a range of 0.1–0.5. This investigation revealed that the force plateau of NiTi archwire occurred at positive slope, with steeper gradient recorded on the model with a higher friction coefficient. This implies that lower contact friction is preferable in a bracket system to preserve the force plateau characteristic.

Keywords

Nickel-titanium archwire • Bracket friction
Force-deflection • Bending

Introduction

In fixed appliance therapy, the force-induced movement of a tooth is obtained from the force being released during the recovery of the deflected archwire. The early discovery of this therapy considered the usage of stainless steel archwire, before the orthodontist shifted to NiTi archwire for its

superelastic property. The superelasticity allows the NiTi archwire to deliver light and constant force over a large magnitude of bending activation—the suitable force characteristics to move a highly displaced tooth during the initial stage of orthodontic treatment. In today's market, the dental bracket is manufactured from several materials, ranging from stainless steel to ceramic and plastic. The development of brackets from ceramic and plastic is to meet aesthetic demands requested by the patients, as these materials promote a translucent look with a color of a tooth. Unfortunately, these types of brackets are reported to induce more sliding resistance upon the sliding of archwire along the bracket slot [1].

In orthodontic studies, the force delivery behaviors of NiTi archwire under bending loads are evaluated through the force-deflection curve. Although there are two force levels on the force-deflection curve, the unloading curve is in fact the portion of interest because it reflects the magnitude of force released by the archwire to the teeth [2]. Until today, the force-deflection curves were obtained over different bending models, including cantilever [3], three-point bending [4], and modified three-point bending [5]. It is reported that in cantilever and three-point bending tests, the force released by NiTi archwire is characterized by an unloading plateau [6]. However, the incorporation of a bracket attachment in the modified three-point bending model is found to alter the force plateau into a slope [7] due to the generation of contact friction between the wire and the bracket.

The contact friction in archwire sliding mechanics can be classified into classic friction and binding [8]. Classic friction refers to sliding resistance created by elastomer ligatures when it drives the archwire against the base of the bracket slot. Meanwhile, binding refers to friction developed when the archwire is bent, with the magnitude of friction increases as the curvature of the bend increases [9]. During tooth movement, along with sliding of the wire on the adjacent brackets, the deactivation force of NiTi archwire is partially used to overcome the binding friction developed due to the bend of the wire, hence lowering the magnitude of effective

M. F. Razali · A. S. Mahmud (✉)

Nanofabrication and Functional Materials Research Group,
School of Mechanical Engineering, Universiti Sains Malaysia,
Engineering Campus, 14300 Penang, Malaysia
e-mail: abdu@usm.my

M. F. Razali
e-mail: fauzinizam88@gmail.com

force to induce tooth movement [5]. Studies pertaining to binding friction have been carried over various combinations of bracket materials and NiTi wire sizes. It is reported that binding increases with an increase in the size of the archwire [10] and the friction coefficient (μ) of the meeting surfaces [11].

Although numerous studies have evaluated the binding magnitude with different archwire-bracket combinations, the influence of contact friction on the force-deflection behaviors of NiTi archwire during bending has remained unreported. Therefore, the objective of this work is to evaluate the force-deflection released by the superelastic NiTi wire upon couples with different bracket material. This investigation was conducted using computational technique by developing a three-dimensional finite-element model that simulated the bending of archwire at varied contact friction. This approach allows a direct control of the friction coefficient encountered for different wire-bracket combinations. A common combination of appliances for a standard configuration of leveling was considered for the evaluation of the force-deflection. The analysis focused on the magnitude and slope of the force during the deactivation course. This finding may assist orthodontists in selecting the best bracket material to comply with the light and constant force criteria suggested for effective tooth movement.

Methodology

Experimental Testing

The force-deflection of superelastic NiTi archwires in the bracket system was investigated by using a modified three-point bending test as described in [5]. The concept of this setup incorporates the effect of contact friction towards force-deflection behavior during bending. This setup considered three aligned brackets, with the central and adjacent brackets mounted on a movable indenter and fixed supports, respectively. Three brackets with a slot size of 0.46×2.80 mm were selected for their zero torque and angulation design. The pairing of 0.4 mm wire with the 0.46 mm-slot bracket provides sufficient clearance for the free sliding of the wire [12]. No ligature was installed in securing the wire specimen inside the bracket slot to avoid the unnecessary friction. As shown in Fig. 1, the interbracket distance (IBD) was set to 7.5 mm, and the specimen was deflected to 4.0 mm by moving the indenter vertically downwards at a rate of 1.0 mm/min. A heating chamber was used to maintain the testing environment at 36 °C. This bending test was repeated twice for consistency purposes, and the curves were directly compared with the numerical result for validation.

A sliding test was conducted to determine the static friction coefficient between NiTi wire and stainless steel

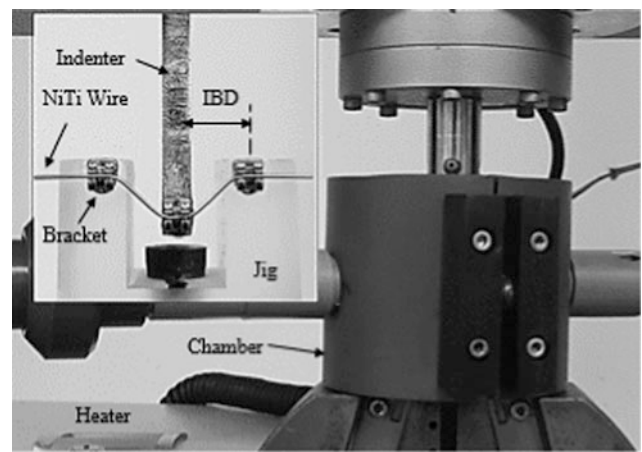


Fig. 1 Modified three-point bending setup equipped with a heating chamber

brackets, which was later used to define the frictional properties in the numerical model. The sliding test was carried out by using a Ducom TR-20 pin-on-disk tribometer. In order to allow greater clearance between the archwire and bracket slot, a 0.40×0.56 mm NiTi archwire and a 0.56 mm bracket slot were selected for the test.

A straightened wire specimen was glued to the surface of a movable sliding plate and aligned against the fixed bracket slot. The sliding test began with applying a 2 kg (19.62 N) dead weight on the loading pan, which subsequently caused the bracket to press the archwire. Then, the NiTi wire was reciprocally slid along the slot at a speed of 1 mm/sec for 4 mm displacement. The friction coefficient was obtained by dividing the friction data with the applied load. The sliding test was repeated three times with new archwires and brackets for each run.

Finite Element Modeling

The finite-element model and the force analysis were performed using a commercial finite-element analysis package of Abaqus/Standard version 6.12-1 in combination with UMAT/Nitinol subroutine. The subroutine has been developed based on the constitutive model of superelastic NiTi alloys by Auricchio and Taylor [13]. The material data that constitutes the mechanical properties and shape memory deformation behaviors of the specimen used in the subroutine are tabulated in Table 1. Each parameter in this table was measured and calculated from the uniaxial tensile stress-strain curve. Additionally, since the compression test on such a small wire specimen is impossible, the start of transformation stress in compression (σ_{SCL}) was set to be 1.2 times higher than the start of transformation stress in tension (σ_{SL}) [14].

Table 1 Mechanical properties and shape memory deformation behaviors of NiTi archwire measured from the uniaxial stress-strain curve

Parameter	Description	Value (unit)
E_A	Austenite elasticity	44 (GPa)
(ν_A)	Austenite Poisson's ratio	0.33
E_M	Martensite elasticity	23 (GPa)
(ν_M)	Martensite Poisson's ratio	0.33
(ϵ_L)	Transformation strain	0.06
$(\delta\sigma/\delta T)_L$	Stress rate during loading	6.7 (MPa/°C)
σ_{SL}	Start of transformation loading	377 (MPa)
σ_{EL}	End of transformation loading	430 (MPa)
T_0	Reference temperature	26 (°C)
$(\delta\sigma/\delta T)_U$	Stress rate during unloading	6.7 (MPa/°C)
σ_{SU}	Start of transformation unloading	200 (MPa)
σ_{EU}	End of transformation unloading	140 (MPa)
σ_{SCL}	Start of transformation stress in compression	452 (MPa)

A nonlinear finite-element model of modified three-point bending was developed to evaluate the force-deflection behavior of the NiTi archwire prior to the displacement of the middle bracket. The 30 mm length specimen was modeled by using 72,000 linear hexahedral elements with reduced integration (C3D8R). The bracket was modeled by using a bilinear rigid quadrilateral element (R3D4) with the actual slot dimensions of 0.46×2.80 mm. Figure 2 illustrates the assembly of the wire and the brackets, with a center-to-center distance between the brackets of 7.5 mm. Each bracket was assigned to its own reference point (RP), so that the boundary condition set to the reference point could be applied to the entire bracket. The middle bracket was set to be free to move only along the vertical axis and the displacement rate was controlled at 1.0 mm/min ($U_x = U_z = 0$). The adjacent brackets were fixed in all displacement directions ($U_x = U_y = U_z = 0$).

The contact between the wire and the rigid brackets was modeled using the finite sliding, surface-to-surface formulation. For validation with the experimental work, a friction coefficient of 0.27 (acquired from the sliding test) was defined at the possible contacted surfaces. Then, the simulation was expanded to different friction conditions by varying the coefficient values from 0.1 to 0.5. In detail, the

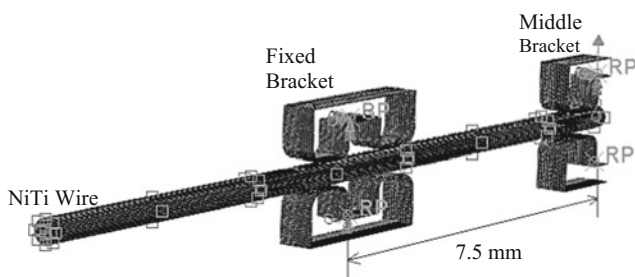


Fig. 2 Finite element model for the modified three-point bending test

coefficient values of 0.1–0.3 and 0.4–0.5 reflected the friction coefficients range of NiTi wire when in contact with stainless steel [15] and ceramic [16] brackets, respectively. All simulations were conducted at a constant temperature of 36 °C. The force-deflection result was attained by requesting the vertical reaction force (RF2) and displacement (U2) at the reference point of the middle bracket.

Results and Discussion

Figure 3 displays the experimental results of frictional force and friction coefficient established from the sliding test. The static friction was observed at the beginning of the wire movement as indicated by the maximum frictional peak. Beyond static friction are the peaks of kinetic friction that fluctuated at a slightly lower magnitude. In brief, the static friction coefficient was averaged at 0.27. This coefficient

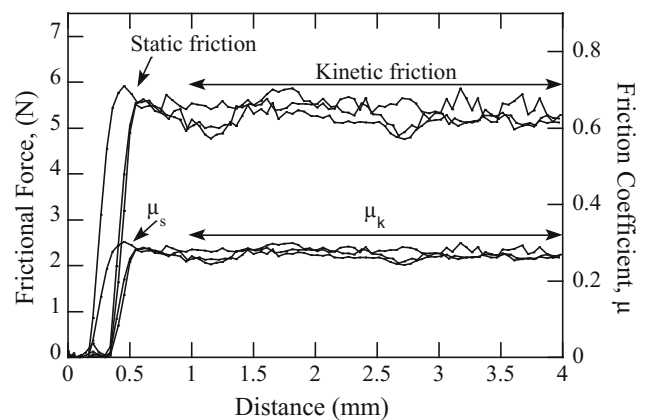


Fig. 3 Plot of frictional force and friction coefficient along the 4.0 mm sliding distance

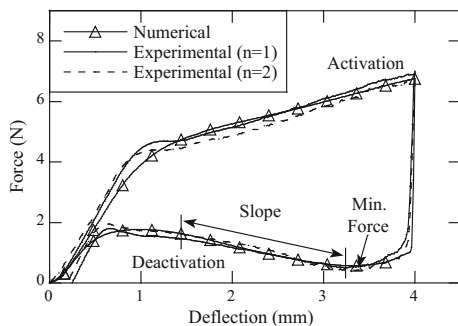


Fig. 4 Force-deflection curve of NiTi archwire bent in three-bracket configuration at 36 °C

value falls within the expected coefficient range for stainless steel bracket coupling, as reported in [15]. It was also acknowledged that a small variation was registered in the coefficients of static friction (standard deviation of 0.20).

Figure 4 compares the force-deflection curve obtained from the numerical and experimental work. A relatively accurate agreement in force magnitude was observed between the experimental and the numerical curves, as indicated by the small discrepancy of force magnitude (0.2 N) at 4.0 mm deflection. Since the test was performed over the austenite finish temperature, the numerical results portrayed the exact superelastic expression represented by the full deflection recovery. As for the experimental result, a small magnitude of residual elongation was observed, indicating a small volume of the specimen being plastically deformed during the activation sequence.

In orthodontic practices, the actual force delivered to the periodontium is represented by the deactivation curve of the force-deflection. Since the deactivation curve exhibited over a slope trend, the evaluation of the effective force for tooth movement was focused on the magnitude of minimum force and the slope of the curve. As illustrated in Fig. 4, the minimum force of the archwire is measured at the valley of the deactivation curve, of which the deflection distance is 3.2 mm. Meanwhile, the slope of the force was measured from the best linear region along the deactivation curve, as indicated by the arrow in the figure. This gradient force behavior of superelastic NiTi wire during bending in the bracket system was consistently correlated to the linear increase of friction at the wire-bracket interface [17]. The valley at the onset of the deactivation curve indicates that a greater portion of the force was utilized to encounter the friction.

The force-deflection curves of the archwire at various friction coefficients are plotted in Fig. 5. At $\mu_s = 0.1$, the bending deformation behavior displayed a typical superelastic curve, such as indicated by the flat force plateaus on both wire activation and deactivation. The activation plateau corresponded to stress-induced martensitic transformation (SIMT), while the deactivation plateau at a lower force level denoted

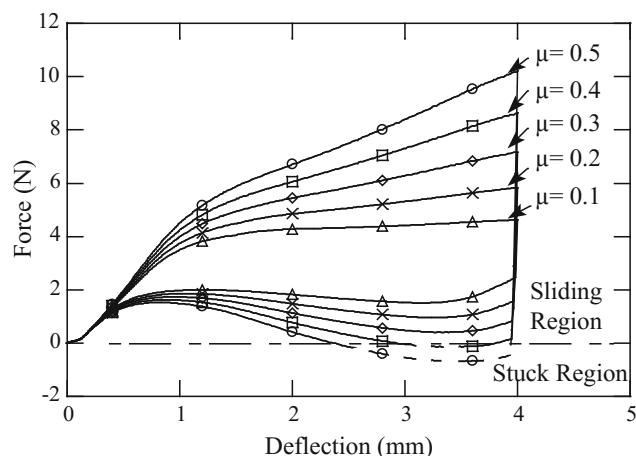


Fig. 5 Numerical results of the force-deflection curves at various friction coefficients

the reversed transformation of the wire phase at the onset of stress removal. As the friction coefficient increased, the stress plateau level also increased proportionally. The activation plateau stress increased in positive slope, but the deactivation plateau increased in negative slope. This force slope is related to the variation of binding created at the contact location between the wire curvature and the bracket edges [9].

Additionally, it is also interesting to highlight that the increment in coefficient value delayed the deactivation curve to a lower force level. For the case in which friction coefficients were 0.4–0.5, the minimum force was plummeted beyond the zero force level. The zero force marks the end of the sliding mechanics of the archwire as the spring-back force was no longer capable to overcome the overpowered contact friction (binding) at the adjacent bracket slot. Therefore, the archwire was subsequently stuck at the onset of deactivation. If one were to translate this phenomenon from a clinical perspective, no movement of the tooth will be induced until the wire can be released from its stuck position.

For this simulation, one should note that the middle bracket incorporated in the model was set to return to its original position at the end of the deactivation mode. Therefore, the negative force magnitude shall be denoted as the minimum force required to surpass the contact friction, hence allowing the archwire to slide again for the remaining deflection. This similar zero force behavior was reported previously prior to the deactivation of the NiTi archwire from 6.0 mm bracket displacement [18].

The magnitude of the minimum force and the deactivation slope measured in Fig. 5 is plotted in Fig. 6. It was recognized that the increase of coefficient values from 0.1–0.5 has increased the slope of the deactivation curve from 0.31 N/mm to 1.10 N/mm, respectively. This slope rate signified that the high friction coefficient case would lead to superior force changes as the deflection recovers; a condition which is

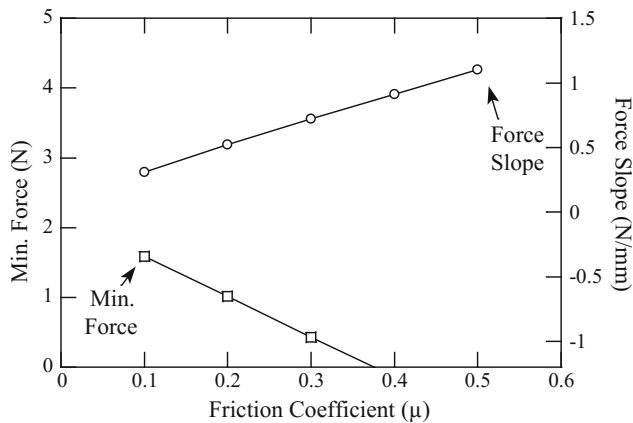


Fig. 6 Variation of minimum force and deactivation slope at various friction coefficients

unsuitable to induce tooth movement. It can also be seen that the minimum force decreased linearly from 1.60 to 0.42 N when the friction coefficient was increased from 0.1 to 0.3. Noted that the data points of minimum force for cases with a friction coefficient higher than 0.4 were not included in this figure due to their values being below zero. This observation signified that the spring-back potential of the archwire during the deactivation was used to overcome the high contact friction, thus hindering further recovery. In this regard, it is recommended that the friction coefficient between the wire and bracket should be limited to lower than 0.3 for effective tooth movement. Subsequently, the use of ceramic brackets is highly not recommended due to the fact the contact friction between ceramic and NiTi archwire can be higher than 0.5 due to its rougher surface morphology [11]. Thus, the orthodontist is strongly suggested to consider the stainless steel bracket ($\mu \leq 0.3$) for the leveling treatment, as this bracket promotes positive forces with a minimum force variation.

Conclusion

The main findings are summarized below:

1. The binding friction increased proportionally as the wire deflection magnitude increased.
2. The bending of NiTi archwire at friction coefficients higher than 0.4 reduced the deactivation force to zero value, and thus would inhibit further tooth movement.

Acknowledgements The authors are grateful for the financial support provided by Universiti Sains Malaysia under the grant RUI 1001/PMEKANIK/814244.

References

1. Williams CL, Khalaf K (2013) Frictional resistance of three types of ceramic brackets. *J Oral Maxillofac Res* 4:e3
2. Segner D, Ibe D (1995) Properties of superelastic wires and their relevance to orthodontic treatment. *Eur J Orthod* 17:395–402
3. Pesce RE et al (2014) Evaluation of rotational control and forces generated during first-order archwire deflections: a comparison of self-ligating and conventional brackets. *Eur J Orthod* 36:245–254
4. Gatto E et al (2013) Load-deflection characteristics of superelastic and thermal nickel-titanium wires. *Eur J Orthod* 35:115–123
5. Nucera R et al (2014) Influence of bracket-slot design on the forces released by superelastic nickel-titanium alignment wires in different deflection configurations. *Angle Orthod* 84:541–547
6. Bartzela TN, Senn C, Wichelhaus A (2007) Load-deflection characteristics of superelastic nickel-titanium wires. *Angle Orthod* 77:991–998
7. Badawi HM et al (2009) Three-dimensional orthodontic force measurements. *Am J Orthod Dentofac Orthop* 136:518–528
8. Burrow SJ (2009) Friction and resistance to sliding in orthodontics: a critical review. *Am J Orthod Dentofacial Orthop* 135:442–447
9. Hamdan A, Rock P (2008) The effect of different combinations of tip and torque on archwire/bracket friction. *Eur J Orthod* 30:508–514
10. Major PW et al (2014) Effect of wire size on maxillary arch force/couple systems for a simulated high canine malocclusion. *J Orthod* 41:285–291
11. Doshi UH, Bhad-Patil WA (2011) Static frictional force and surface roughness of various bracket and wire combinations. *Am J Orthod Dentofac Orthop* 139:74–79
12. Proffit WR, Fields Jr HW, Sarver DM (2014) Contemporary orthodontics. Elsevier Health Sciences
13. Auricchio F, Taylor RL (1997) Shape-memory alloys: modelling and numerical simulations of the finite-strain superelastic behavior. *Comput Methods Appl Mech Eng* 143:175–194
14. Auricchio F, Sacco E (1999) A temperature-dependent beam for shape-memory alloys: Constitutive modelling, finite-element implementation and numerical simulations. *Comput Methods Appl Mech Eng* 174:171–190
15. Whitley JQ, Kusy RP (2007) Influence of interbracket distances on the resistance to sliding of orthodontic appliances. *Am J Orthod Dentofac Orthop* 132:360–372
16. Kusy RP, Whitley John Q (1990) Coefficients of friction for arch wires in stainless steel and polycrystalline alumina bracket slots. I. The dry state. *Am J Orthod Dentofac Orthop* 98:300–312
17. Thalman TD (2008) Unloading behavior and potential binding of superelastic orthodontic leveling wires. M.Sc. thesis, Saint Louis University
18. Baccetti T et al (2009) Forces produced by different nonconventional bracket or ligature systems during alignment of apically displaced teeth. *Angle Orthod* 79:533–539